

# Experimental and Kinetic Studies on Tobacco Pyrolysis under a Wide Range of Heating Rates

Yanfei Mu, Yuhan Peng, Xiaodong Tang, Jie Ren, Jiangkuan Xing, Kun Luo,\* Jianren Fan, and Ke Zhang\*



Cite This: *ACS Omega* 2022, 7, 1420–1427



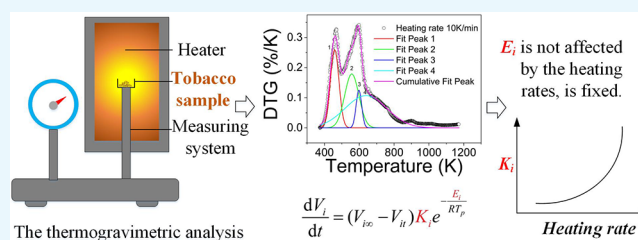
Read Online

ACCESS |

Metrics & More

Article Recommendations

**ABSTRACT:** In the present work, experimental and kinetic studies are conducted to explore and model tobacco pyrolysis characteristics under a wide range of heating conditions. First, thermal decomposition processes of a tobacco sample were investigated using thermogravimetric analysis/difference thermogravimetry (TGA/DTG) experiments under a wide range of heating rates (10–500 K/min), and the TGA/DTG profiles were compared to highlight the effect of heating rate on the pyrolysis characteristics. The results showed that the tobacco sample was sufficiently devolatilized at 1173.15 K (900 °C) and the final volatiles yields were not sensitive to the heating rate. Moreover, it was illustrated that the DTG curve presents a polymerization trend with the increase in heating rate. Then, kinetic parameters, including total component mass fraction, preexponential factor, and activation energy, were derived by deconvolution from TG/DTG profiles for each component with a one-step kinetic framework, and the correlations between kinetic parameters and heating rates were further explored and modeled. The results illustrated that four subpeaks can be found in the deconvolution, indicating the four components (volatile components, hemicellulose, cellulose, and lignin). In addition, the activation energy of each component was found to be insensitive with heating rate (with standard deviation less than 20%). Therefore, an average activation energy was used for each component to avoid the compensation effect and a power correlation between the heating rate and the preexponential factor could be found. *A posteriori* analysis also confirmed the validity of this correlation.



## 1. INTRODUCTION

It is generally believed that a series of complex chemical reactions occur during cigarette smoking and the majority of organic smoke components are formed in the pyrolysis region.<sup>1,2</sup> Moreover, the pyrolysis products of tobacco have the most significant impact on sensory properties.<sup>3–5</sup> Therefore, it needs to have a more in-depth understanding of thermal decomposition processes for the research, development, production, and maintenance of cigarettes, according to modulation methods and harm reduction requirements.<sup>6–9</sup> There are different reaction stages during tobacco smoking, such as smoldering and puffing. The span of the local heating rate is large for different regions and burning conditions,<sup>10–12</sup> where the range of heating rate is about 5–500 K/min, and the highest temperature is about 1173 K.<sup>13,14</sup> Previous studies show that the heating rate would significantly influence the pyrolysis behavior of solid fuels.<sup>15,16</sup> Therefore, it is of great significance to study the pyrolysis process of the tobacco sample at different heating rates and obtain reliable kinetic data to establish a cigarette combustion mathematical model.

Thermogravimetric analysis/difference thermal gravimetry test (TGA/DTG) is a general term for determining the tested substance's mass change under certain temperature-pro-

grammed conditions. Because of its simple principle and convenient operation, it has been widely used to study the reaction kinetics equation of coal, biomass, and other solid fuels in the process of thermal decomposition.<sup>17–22</sup> TGA/DTG is also convenient for the research of the tobacco pyrolysis process. For tobacco, more attention is paid to predict yields and evolution patterns of volatile tobacco products. Wójtcowicz has established a tobacco pyrolysis model based on first-order kinetic expressions with a Gaussian distribution of activation energies by the TGA method of low heating rates (10, 30, and 100 K/min, from 423.15 to 1173.15 K).<sup>23</sup> According to TGA (5, 10, 20, 40, and 80 K/min, from 373.15 to 900 K) experimental results, Weixuan divides the pyrolysis process of tobacco waste into four stages and calculates the corresponding stages' activation energy.<sup>24</sup> Deqing studied the effect of four potassium inorganic and organic salts on the pyrolysis kinetics of cigarette

**Received:** November 1, 2021  
**Accepted:** December 10, 2021  
**Published:** December 21, 2021



paper in a temperature range of 303.15–1173.15 K at a heating rate of 20 K/min under inert atmosphere and thought that potassium salts decreased the activation energy remarkably.<sup>25</sup> Federica used TGA–Fourier transform infrared (TGA-FTIR) (10 K/min, from 298.15 to 823.15 K) to identify and quantitatively analyze the volatile compounds formed during the thermal degradation of tobacco substrate and get emission profiles of some key components of evolved gases.<sup>26</sup> Previous studies mainly studied the pyrolysis of cigarettes at a low heating rate but less at a high heating rate.<sup>23–31</sup> This article will use experimental methods to study a broader range of heating rates and further establish a pyrolysis model at a wide heating rate based on the TGA/DTG test results (10 K–500 K/min). It can provide a more accurate kinetic module for establishing CFD simulation of the cigarette smoking process, which is for improving product design and evaluation in the tobacco industry.

## 2. METHODS

In the present work, experimental and kinetic investigations of the tobacco pyrolysis are conducted, and the detailed approaches are introduced as follows.

**2.1. Experiment.** Thermogravimetric analysis (TGA) is used to analyze and elucidate tobaccos' thermal conversion, with a measure of percent mass loss of sample as a function of the pyrolysis temperature or time. The curve that records the relationship between the mass of this substance and the temperature or time is called the TGA curve, while that records the relationship between the difference in the mass and the temperature or time difference is called the DTG curve. To obtain a more accurate TGA/DTG data of different tobacco samples and eliminate the influence of heat and mass transfer factors such as the increase of internal and external temperature gradient of tobacco sample under a high-temperature rise rate, the delay of internal pyrolysis rate than surface pyrolysis, and the aggregation of pyrolysis gas-phase products, it is necessary to design the experimental conditions of the thermal analysis process reasonably.

**2.1.1. Preparation of Materials.** The chemical composition of the sugar analysis of the tobacco sample is determined by continuous flow analysis (CFA), as shown in Table 1. The

**Table 1. Sugar Component of Tobacco Samples**

total sugar (%)	phytoalexins (%)	reducing sugars (%)	chlorine (%)	potassium (%)	total nitrogen (%)
33.08	2.38	28.43	0.45	1.94	1.81

continuous flow analytical method was applied extensively in the tobacco industry as a quick, exact, and batch quantity analysis method. The data of total sugar, reducing sugar, water-soluble sugar, total nitrogen, protein, chlorine, and calcium in tobacco samples can be obtained quickly and accurately.<sup>34–36</sup>

The tobacco sample is crushed by a high-speed pulverizer and passed through a sieve with an aperture of 178  $\mu\text{m}$  (80 mesh). It takes 10 mg of different smoke powder samples and places them in a 100  $^{\circ}\text{C}$  blast oven for 2 h before the pyrolysis test eliminates the moisture. The DTG curves of different sample masses are compared under the same experimental conditions to explore the heat transfer effect in the TG experiment. When the sample mass was reduced from 10.0 mg to 4.0 and 2.0 mg, the DTG curve did not change. Accordingly, such sample mass of 10 mg

was low enough to eliminate the mass transfer limitation and ensure a small Biot number.

The Biot number ( $Bi$ ) of a single tobacco sample particle could be estimated as

$$Bi = \frac{hd}{\lambda} = \frac{10 \text{ W}/(\text{m}^2\cdot\text{K}) \times 178 \times 10^{-6} \text{ m}}{0.112 \text{ W}/(\text{m}\cdot\text{K})} = 0.015893 < 0.1 \quad (1)$$

where  $h$  is the convective heat transfer coefficient. Generally, natural convection's convective heat transfer coefficient ranges from 1 to 10  $\text{W}/(\text{m}^2\cdot\text{K})$ . Here, it is assumed that the convective heat transfer coefficient between the tobacco sample and the surrounding gas convection is 10  $\text{W}/(\text{m}^2\cdot\text{K})$ ;  $d$  is the diameter of tobacco sample particles, 178  $\mu\text{m}$  (80 mesh); and  $\lambda$  is the thermal conductivity of the tobacco sample, measured to be 0.112  $\text{W}/(\text{m}\cdot\text{K})$ . The calculated Biot number ( $Bi$ ) of tobacco sample particles is less than 0.1. The difference between the internal and external temperatures of tobacco particles is less than 5%, which means that the internal temperature of tobacco sample particles is uniform and consistent with the temperature rise curve set by the instrument, which minimizes temperature gradients inside the particles during pyrolysis. Therefore, the influence of heat and mass transfer factors is limited in those experiments.

**2.1.2. Pyrolysis Test Conditions.** The tobacco sample will be heated from 100 to 900  $^{\circ}\text{C}$  under different heating rates (from 10 to 500  $^{\circ}\text{C}/\text{min}$ ) without hold time. A blank experiment was performed under the same conditions before the experiment to eliminate the effect of system error on the experiment result. More than three groups of repeated experiments were carried out at each heating rate, and all of the DTG curves of the repeatability experiment under the same condition coincided.

**2.2. Gauss Peak Fitting.** The pyrolysis process of tobacco is when four components (volatile components, hemicellulose, cellulose, and lignin) are successively separated and escaped.

The software Python's Gauss peak fitting module is used to separate the four components' reaction rate curves from the total DTG curve.<sup>27</sup> The pyrolysis peak temperatures of the four components are set to be consistent with the literature's data,<sup>19,30</sup> and the correlation coefficients  $R^2$  of the relevant results are generally larger than 0.9, indicating that the fitting results are accurate and credible. The proportions of the four components of the tobacco sample are then prepared for pyrolysis kinetic analysis.

**2.3. Pyrolysis Kinetic Analysis.** A model based on first-order reactions with Gauss distributions of activation energies was used to fit the four components' peak data of Section 2.2.<sup>32</sup>

$$\frac{dV_i}{dt} = (V_{i\infty} - V_{it})K_i e^{-E_i/RT_p} \quad (2)$$

where the subscript  $i$  represents four components (volatile components, hemicelluloses, cellulose, lignin) in the pyrolysis process;  $dV_i/dt$  denotes the volatile release rate of component  $i$ ;  $V_{i\infty}$  represents the final yield of component  $i$ , which can be obtained by integrating the DTG curve of component  $i$  after splitting the peak;  $V_{it}$  is the yield of component  $i$  at time  $t$ , which can also be obtained through the DTG curve of component  $i$ ;  $E_i$  is the activation energy of component  $i$ ; and  $T_p$  is the particle temperature.

$$\ln\left(\frac{dV}{(V_{i\infty} - V_{it})dt}\right) = \ln(K_i) - E_i \frac{1}{RT_p} \quad (3)$$

We take logarithm on both sides of eq 2 and calculate the activation energy  $E_i$  and the pre-factor  $K_i$  from the fitted straight line's slope and intercept,<sup>33</sup> as shown in eq 3.

### 3. RESULTS AND DISCUSSION

**3.1. TGA and DTG Results.** TGAs under 11 heating rates have been measured for the tobacco sample. The heating rate ranges from 10 to 500 K/min with an interval of 50 K/min, the moisture has been dried and removed, and the results are shown in Figure 1. It can be seen that from 373.15 K, the temperature

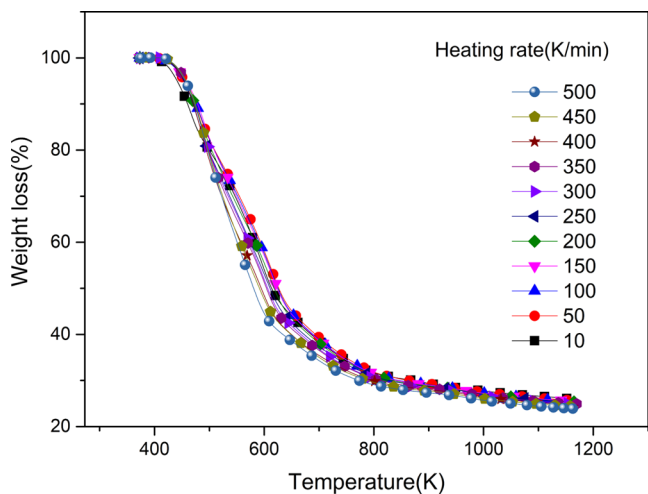


Figure 1. TGA curves at different heating rates.

(or time) starts to increase. Finally, the tobacco sample's mass decreases quickly and the slope of the curve is getting closer to 0 after about 1000 K. The average residual mass of all of the curves is about 24.98%. Therefore, it can be concluded that the pyrolysis of tobacco has been completed at 1173.15 K (900 °C), which is not affected by the heating rate.

The DTG curve shows the relationship between the pyrolysis rate with temperature or time. The different superimposed peaks of the DTG curve are generally caused by different components' content and the pyrolysis characteristics in the reaction process. The different components on the DTG curve can be separated by the Gauss peak fitting method. The tobacco sample's DTG curve is obtained by differentiating the tobacco TGA curve with time or temperature. Figure 2 shows the DTG curves of this tobacco sample under different heating rates. It can be found that as the heating rate increases, the peak value of the DTG curve presents a polymerization phenomenon. For example, at a heating rate of 500 K/min, DTG only has a single-peak shape. On the contrary, there are two obvious peaks when the heating rate is low, and the lower the heating rate, the more obvious the separation of the peaks.

**3.2. Gauss Peak Fitting Method.** To find the possible reason for the polymerization at a high heating rate, the reaction rate curve of four components (volatile components, hemicellulose, cellulose, and lignin) is obtained by Gauss peak fitting of DTG curves. The peak splitting results at a low heating rate are shown in Figure 3. During the pyrolysis of tobacco, four components precipitated successively. Relevant literature<sup>37,40</sup> points out that the pyrolysis temperature range of volatile

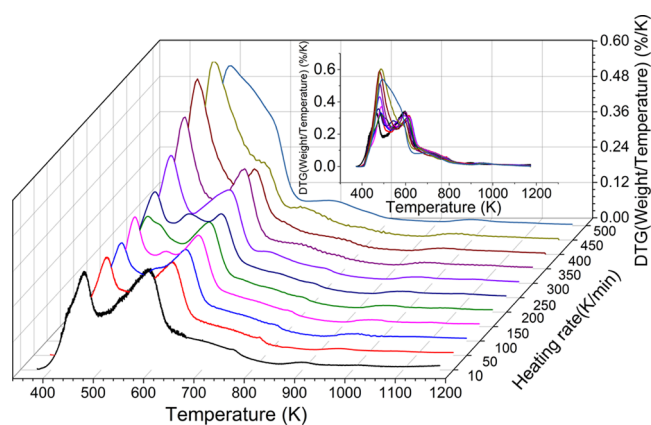


Figure 2. DTG curves at different heating rates.

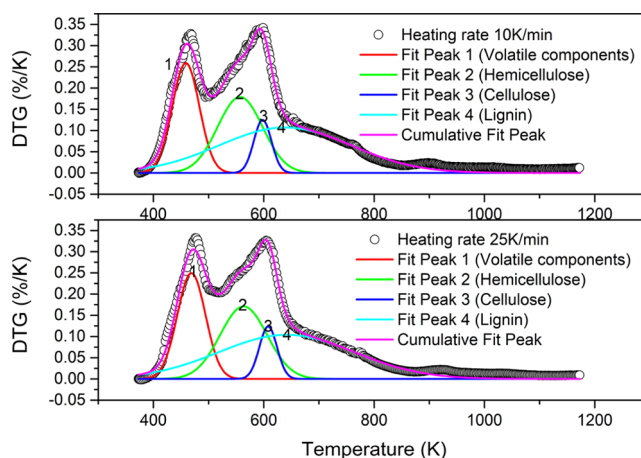


Figure 3. Gauss peak fitting at low heating rates (free fitting).

components is 373–525 K, the pyrolysis temperature range of lignin is 523–773 K, the pyrolysis temperature range of hemicellulose is 498–598 K, and the pyrolysis temperature range of cellulose is 598–648 K. In this experiment, the pyrolysis temperature range of each component is similar to the data in the previous literature, which also verifies the accuracy of the experimental results.

There is an important issue about determining the tobacco ratio of the four components. The ratio of the four components inside the same tobacco sample is fixed and is not affected by heating rate. Here, the component ratio obtained by Gaussian peak fitting at a heating rate of 10 °C/min is used as tobacco components' characteristics. The main reason for this treatment is that the free fitting of the four components' Gauss peaks to the single-peak DTG curve at a high heating rate is nonunique. That is, the four components can be well-fitting to the single-peak DTG curve in different proportions. However, for the DTG curve at low heating rates (such as 10 and 25 K/min), the four components' Gauss peak fitting result is fixed and unique. The relevant result is shown in Figure 3. Furthermore, after fixing the proportion of the four components, a good fitting result can also be obtained by Gauss peak fitting of the 450 or 500 °K/min DTG curve, as shown in Figure 4. Therefore, the peak splitting results at 10 K/min are used to distinguish the characteristics of the tobacco components.

The component proportion of the tomato sample is determined as follows:

- The proportion of volatile components is 22.35%.

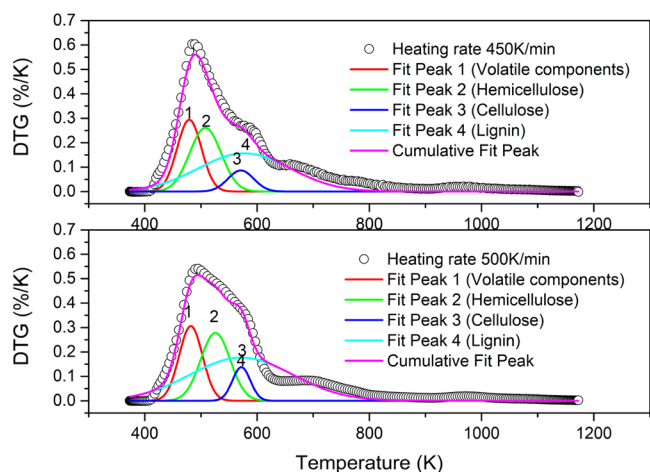


**Figure 4.** Gauss peak fitting at high heating rates (fixed proportion of the four components).

- The proportion of hemicellulose is 25.63%.
- The proportion of cellulose is 6.98%.
- The proportion of lignin is 45.05%.

Furthermore, the DTG curves at different heating rates were fitted by Gaussian fitting under a fixed component ratio condition. As shown in Figure 5, it is found that the peak positions of volatile components move in the high-temperature direction with the increase of heating rate, while the peak positions of hemicellulose, cellulose, and lignin move in the low-temperature direction. There is still a lack of reasonable explanations for temperature drift. The internal reasons for its influence may come from two aspects: heat transfer and kinetics.<sup>37–39</sup> Since the particle diameter of the tobacco sample is less than 178  $\mu\text{m}$  (80 mesh), this section will analyze the deviation of the pyrolysis curve of small-size particles at different heating rates from the perspective of kinetics heat release.

Le Chatelier's principle may explain this phenomenon. Le Chatelier's principle states that if a constraint (such as a change in pressure, temperature, or concentration of a reactant) is applied to a system in equilibrium, the equilibrium will shift to tend to counteract the effect of the constraint. With the increase

of heating rate, the rate of heat accumulation around tobacco particles will increase accordingly, which will promote the endothermic reaction and inhibit the exothermic reaction. Therefore, it is supposed that the reason for the peak positions of volatile components movement is that volatile components' pyrolysis is an exothermic reaction. In contrast, hemicellulose, cellulose, and lignin pyrolysis is an endothermic reaction.

**3.3. Results of Pyrolysis Kinetic Analysis.** Because the sensory characteristics of the tobacco sample are most affected by the physical and chemical characteristics of volatile components, the kinetic parameter calculation method described in Section 2.3 is used to calculate the Gauss peak data of the four components. The purpose is to obtain the kinetic parameter differences such as pre-factor  $K$  and activation energy  $E$  under different heating rates. The order of magnitude of the calculated activation energy is consistent with the research results in the relevant literature.<sup>40–43</sup> It shows that the results of the kinetic parameter parameters in Table 2 are correct.

**Table 2.** Statistics on Tobacco Activation Energy under Different Heating Rates

heating rate (K/min)	volatile components $E_1$ (J/mol)	hemicellulose $E_2$ (J/mol)	cellulose $E_3$ (J/mol)	lignin $E_4$ (J/mol)
10	$6.02 \times 10^4$	$5.55 \times 10^4$	$1.66 \times 10^4$	$2.29 \times 10^4$
50	$6.18 \times 10^4$	$5.23 \times 10^4$	$1.71 \times 10^5$	$2.25 \times 10^4$
100	$6.04 \times 10^4$	$5.01 \times 10^4$	$1.70 \times 10^5$	$2.27 \times 10^4$
150	$6.57 \times 10^4$	$5.01 \times 10^4$	$1.76 \times 10^5$	$2.26 \times 10^4$
200	$5.32 \times 10^4$	$4.24 \times 10^4$	$1.66 \times 10^5$	$2.33 \times 10^4$
250	$6.70 \times 10^4$	$5.52 \times 10^4$	$1.68 \times 10^5$	$2.33 \times 10^4$
300	$7.69 \times 10^4$	$4.47 \times 10^4$	$1.56 \times 10^5$	$2.30 \times 10^4$
350	$8.00 \times 10^4$	$3.78 \times 10^4$	$1.92 \times 10^5$	$2.50 \times 10^4$
400	$8.01 \times 10^4$	$5.42 \times 10^4$	$1.32 \times 10^5$	$2.78 \times 10^4$
450	$7.80 \times 10^4$	$6.57 \times 10^4$	$1.05 \times 10^5$	$2.83 \times 10^4$
500	$8.25 \times 10^4$	$7.04 \times 10^4$	$1.63 \times 10^5$	$2.83 \times 10^4$
average value	$6.96 \times 10^4$	$5.26 \times 10^4$	$1.60 \times 10^5$	$2.45 \times 10^4$
standard deviation	10165.45	9505.76	23 382.80	2411.47
relative deviation	14.60%	18.08%	14.58%	9.84%

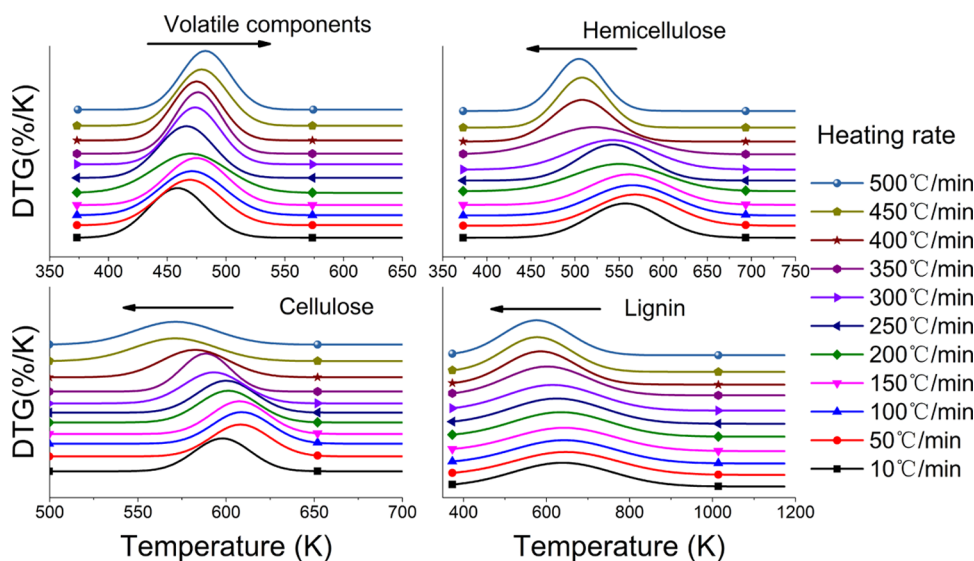


**Figure 5.** Movement trend of the peak position of pyrolysis components.

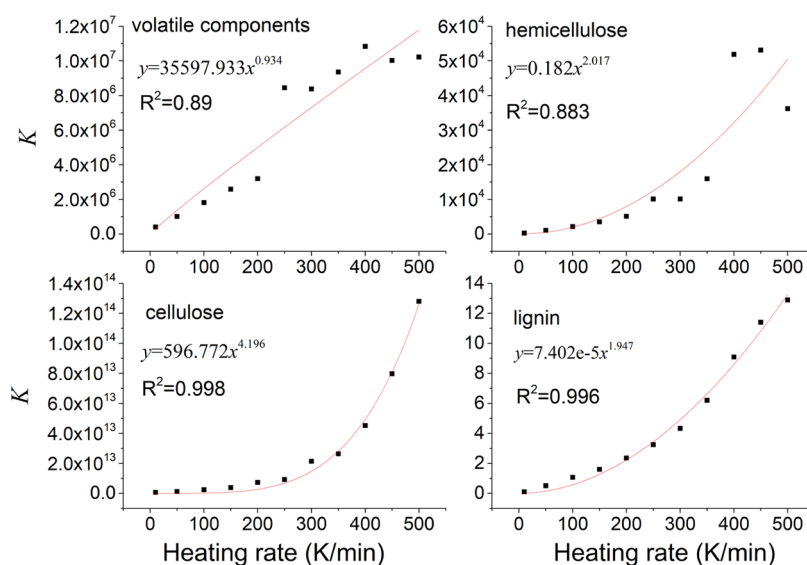


**Figure 6.** Nonlinear relationship between the preexponential factor ( $K_i$ ) of the four components and the heating rate of the tobacco sample. Red lines represent the predictions of the found correlations, and the scatters are the fitted kinetic parameters.

**Table 3.** Power Function Relationship ( $K_i = a \cdot x^b$ ) between the Pre-factor of Tobacco Components ( $K_i$ ) and Heating Rate ( $x$ )

coefficient	volatile components	hemicellulose	cellulose	lignin
$V_\infty$	22.35	25.62	6.98	45.05
$E$	$6.960 \times 10^4$	$5.260 \times 10^4$	$1.600 \times 10^5$	$2.450 \times 10^4$
$a$	$3.560 \times 10^4$	$1.819 \times 10^{-1}$	$5.968 \times 10^2$	$7.402 \times 10^{-5}$
$b$	$9.336 \times 10^{-1}$	$2.017 \times 10$	$4.196 \times 10$	$1.947 \times 10$

It is further found that each tobacco volatile component's activation energy values at different heating rates are relatively concentrated (the variance is small, within 20% of the average; see Table 2). Therefore, by fixing the average activation energy  $E$  of each tobacco sample at different heating rates, the preexponential factor  $K$  is calculated under the condition of fixed activation energy and fit the relationship between the pre-exponential factor and the heating rate numerical methods. The power function (see Figure 6) could be used to well characterize the compensation effect brought by the heating rate. The correlation coefficients of the four components of the tobacco sample are greater than 0.88, which also supports the reasonability of this found correlation.

Based on the previous content, a kinetic model on tobacco pyrolysis under a wide range of heating rates can be established, as shown in formula 1. The correlation coefficient of the model is shown in Table 3, where  $x$  is the heating rate, K/min. The TGA and DTG curves of the tobacco sample can be obtained by solving the differential equation.

**3.4. Model Verification.** A posteriori analysis method is used to compare and verify the TGA data of the tobacco sample under the additional heating rate to verify the correctness of the pyrolysis model proposed in the previous section. The heating rates of additional tests from low to high are 75, 275, and 475 K/min to verify that the model is suitable for a wide range of heating rates.

The following is the pyrokinetic model's verification through the TGA and DTG curve, as shown in Figure 7. The model calculation results of four components (volatile components, hemicellulose, cellulose, and lignin) are solid curves obtained by solving eq 1 and using Table 3. The DTG cumulative result is obtained after the superposition of the four components. It can be found that the model calculation results capture the

dispersion and aggregation of the component peaks. For example, at the 75 K/min heating rate, the DTG curve has two peaks. On the contrary, at the heating rate of 475 K/min, the DTG curve has only one peak by polymerization.

The TGA curve calculated by the model is compared with the experimental results. It can be found that the TGA curve calculated by the model is all small in the latter half than the experimental results among the three sets of results, which may be because the latter half of the DTG curve peak was ignored when the Gaussian peaks were divided. Besides the error, the TGA curve calculation result is very close to the test result and the correlation coefficient is greater than 0.99.

## 4. CONCLUSIONS

In the present work, TGA/DTG tests are conducted for a tobacco sample to find the effect of heating rate on the tobacco pyrolysis behavior and kinetic modeling. The main conclusions are summarized as follows:

- (1) The pyrolysis reaction of tobacco samples can start at a lower temperature of 375.13 K and ends after about 1173.15 K. The pyrolysis residual mass is about 24.98% and is not greatly affected by the heating rate.
- (2) As the heating rate increases, the peak location of the DTG curve presents a polymerization phenomenon. Specifically, the DTG curves have a multipeak shape at a low heating rate, but only have a single peak at a high heating rate. The reason maybe that pyrolysis of volatile components is an exothermic reaction, while the pyrolysis reactions of hemicellulose, cellulose, and lignin are endothermic reactions in an inert atmosphere.
- (3) For DTG curves at low heating rates, the results of the Gauss peak fitting are unique. Moreover, a good fit result

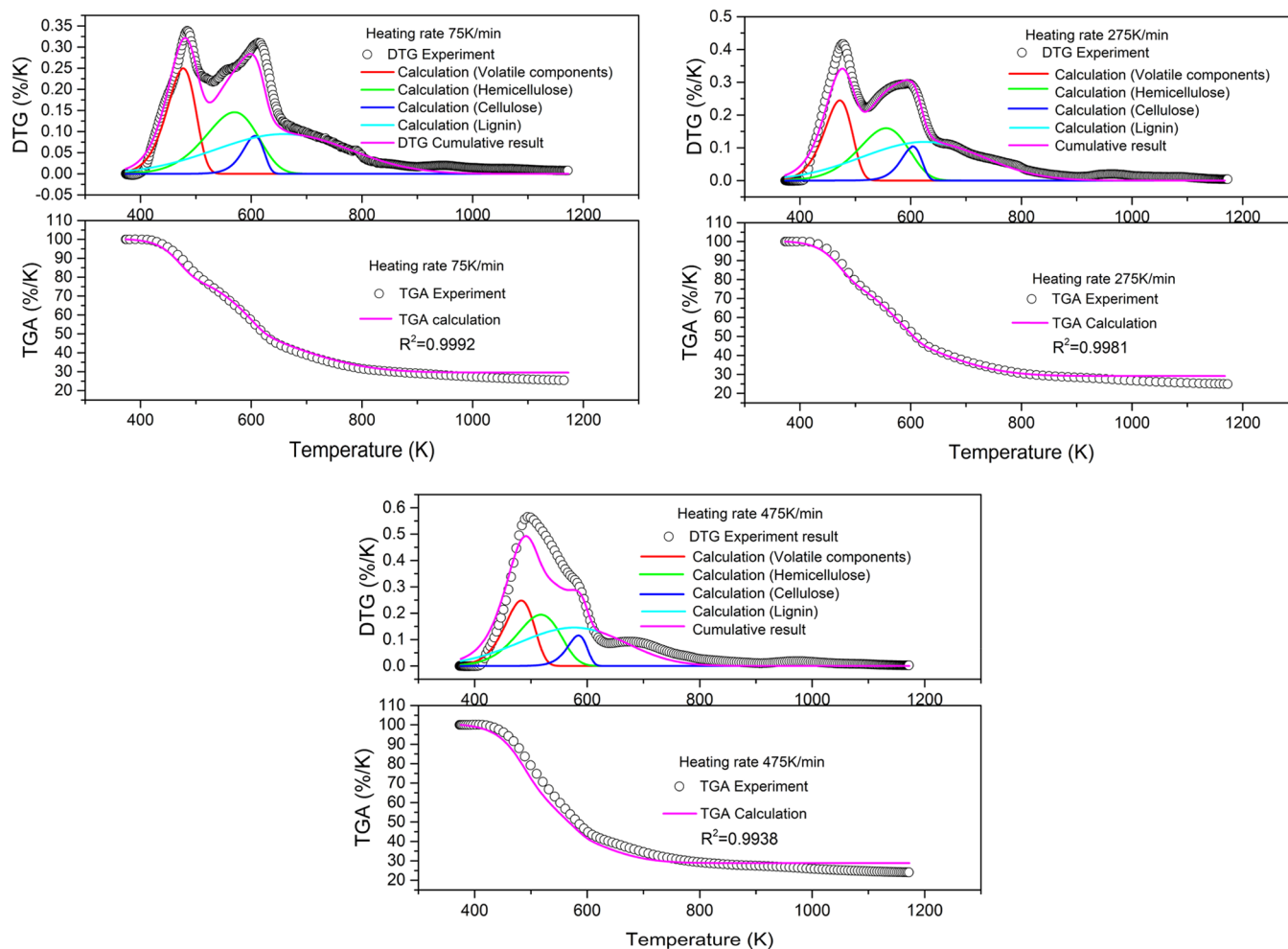


Figure 7. Comparison between model calculation results and experiment results.

can also be obtained by Gauss peak fitting of DTG curves at high heating rates when fixing the four components (volatile components, hemicellulose, cellulose, and lignin), which is the same as the components with DTG curves at low heating rates.

- (4) The statistical results show that the activation energy of tobacco is less affected by the wide range of heating rates. After fixing the activation energy, the power function can characterize the relationship between the heating rate and the preexponential factor. Then, a kinetic model on tobacco pyrolysis under the wide range of heating rates is established. Finally, experiment results and calculation results are compared to verify the kinetic model's validity on tobacco pyrolysis under a wide range of heating rates.

The kinetic model on tobacco pyrolysis can provide relevant pyrolysis parameters for cigarette numerical simulation and be applied to the technical field of cigarette harm reduction and coke reduction and guide the design of heat, not burn tobacco products.

## AUTHOR INFORMATION

### Corresponding Authors

**Kun Luo** – State Key Laboratory of Clean Energy Utilization, Zhejiang University, Hangzhou 310085, P. R. China; [orcid.org/0000-0003-3644-9400](https://orcid.org/0000-0003-3644-9400); Phone: 86-0571-87951764; Email: [zjulk@zju.edu.cn](mailto:zjulk@zju.edu.cn)

**Ke Zhang** – Zhengzhou Tobacco Research Institute of CNTC, Zhengzhou 450001, P. R. China; Email: [hfzhangke@126.com](mailto:hfzhangke@126.com)

### Authors

**Yanfei Mu** – State Key Laboratory of Clean Energy Utilization, Zhejiang University, Hangzhou 310085, P. R. China

**Yuhan Peng** – China Tobacco Zhejiang Industrial Co., Ltd., Hangzhou 310088, P. R. China

**Xiaodong Tang** – China Tobacco Zhejiang Industrial Co., Ltd., Hangzhou 310088, P. R. China

**Jie Ren** – State Key Laboratory of Clean Energy Utilization, Zhejiang University, Hangzhou 310085, P. R. China

**Jiangkuan Xing** – State Key Laboratory of Clean Energy Utilization, Zhejiang University, Hangzhou 310085, P. R. China; [orcid.org/0000-0002-2423-5627](https://orcid.org/0000-0002-2423-5627)

**Jianren Fan** – State Key Laboratory of Clean Energy Utilization, Zhejiang University, Hangzhou 310085, P. R. China; [orcid.org/0000-0002-6332-6441](https://orcid.org/0000-0002-6332-6441)

Complete contact information is available at: <https://pubs.acs.org/10.1021/acsomega.1c06122>

### Notes

The authors declare no competing financial interest.

## ACKNOWLEDGMENTS

The authors are grateful for support from Zhejiang University–Zhejiang China Tobacco Joint Laboratory Fund (grant no. K-20201802) and the Science Foundation of China Tobacco Zhejiang Industrial (grant no. ZJZY2021A009).

## REFERENCES

- (1) Baker, R. R.; Bishop, L. J. The pyrolysis of tobacco ingredients. *J. Anal. Appl. Pyrolysis* **2004**, *71*, 223–311.
- (2) Baker, R. R. The kinetics of tobacco pyrolysis. *Thermochim. Acta* **1976**, *17*, 29–63.
- (3) Li, J.; Cao, J.; Lu, X.; Xia, Y.; Li, Z.; Wang, Y.; Mou, D. Impact of meteorological factors on aroma type and aroma note of flue-cured tobacco in China. *Yancao Keji* **2015**, *48*, 12–19.
- (4) Zhou, S.; Ning, M.; Xu, Y.; Ge, S.; Shu, J.; Wang, C.; Tian, Z.; Hu, Y.; Tao, F. Effects of ammonium polyphosphate on pyrolysis-combustion characteristics and sensory quality of paper-making process reconstituted tobacco sheet. *Yancao Keji* **2013**, 61–66.
- (5) Zhou, S.; Wang, X.; He, Q.; Zhang, Y.; Li, Z.; Tian, Z.; Chen, K.; She, S.; Xu, Y.; Ning, M. Recent advances in detection and analysis technologies relating to combustion and pyrolysis of tobacco and tobacco products. *Zhongguo Yancao Xuebao* **2017**, *23*, 130–142.
- (6) Brunnemann, K. D.; Masaryk, J.; Hoffmann, D. Role of Tobacco Stems in the Formation of N-Nitrosamines in Tobacco and Cigarette Mainstream and Sidestream Smoke. *J. Agric. Food Chem.* **1983**, *31*, 1221–1224.
- (7) Seeman, J. I.; Dixon, M.; Haussmann, H. J. Acetaldehyde in mainstream tobacco smoke: Formation and occurrence in smoke and bioavailability in the smoker. *Chem. Res. Toxicol.* **2002**, *15*, 1331–1350.
- (8) Fried, N. D.; Gardner, J. D. Heat-not-burn tobacco products: An emerging threat to cardiovascular health. *Am. J. Physiol.: Heart Circ. Physiol.* **2020**, *319*, H1234–H1239.
- (9) Yu, L.; Cheng, J.; Cui, X.; Wang, J. Province-specific smoking-attributable cancer mortality in China 2013. *Tob. Induc. Dis.* **2020**, *18*, No. 49.
- (10) Pütin, A. E.; Önal, E.; Uzun, B. B.; Özbay, N. Comparison between the “slow” and “fast” pyrolysis of tobacco residue. *Ind. Crops Prod.* **2007**, *26*, 307–314.
- (11) Müller, B. H. Degradation kinetics of tobacco-survey by fast thermogravimetry analysis. *J. Anal. Appl. Pyrolysis* **1993**, *25*, 273–283.
- (12) Liao, J.; Li, Q.; Chen, G.; Deng, X.; Hu, Z.; Chen, X.; Li, Y. Effects of heating rate on fast pyrolysis of cut filler of cigarette. *Yancao Keji* **2016**, *49*, 44–50.
- (13) Muramatsu, M.; Umemura, S.; Okada, T. A mathematical model of evaporation-pyrolysis processes inside a naturally smoldering cigarette. *Combust. Flame* **1979**, *36*, 245–262.
- (14) SAIDI, M. S.; HAJALIGOL, M. R.; RASOULI, F. Numerical simulation of a burning cigarette during puffing. *J. Anal. Appl. Pyrolysis* **2004**, *72*, 141–152.
- (15) Xing, J.; Bai, Y.; Zhao, C.; Gao, Z.; Wang, H. Numerical Studies of Coal Devolatilization Characteristics with Gas Temperature Fluctuation. *Energy Fuels* **2018**, *32*, 8760–8767.
- (16) Xing, J.; Luo, K.; Pitsch, H.; Wang, H.; Bai, Y.; Zhao, C.; Fan, J. Predicting kinetic parameters for coal devolatilization by means of Artificial Neural Networks. *Proc. Combust. Inst.* **2019**, *37*, 2943–2950.
- (17) Zhao, H.; Yan, H.; Zhang, C.; Sun, B.; Zhang, Y.; Dong, S.; Xue, Y.; Qin, S. Thermogravimetry study of pyrolytic characteristics and kinetics of the giant wetland plant *Phragmites australis*. *J. Therm. Anal. Calorim.* **2012**, *110*, 611–617.
- (18) Ceylan, S.; Kazan, D. Pyrolysis kinetics and thermal characteristics of microalgae *Nannochloropsis oculata* and *Tetraselmis* sp. *Bioresour. Technol.* **2015**, *187*, 1–5.
- (19) Skreiberg, A.; Skreiberg, O.; Sandquist, J.; Sørum, L. TGA and macro-TGA characterisation of biomass fuels and fuel mixtures. *Fuel* **2011**, *90*, 2182–2197.
- (20) Czajka, K.; Kisiela, A.; Morón, W.; Ferens, W.; Rybak, W. Pyrolysis of solid fuels: Thermochemical behaviour, kinetics and compensation effect. *Fuel Process. Technol.* **2016**, *142*, 42–53.
- (21) Zhu, Y. L.; Huang, H.; Ren, H.; Jiao, Q. J. Kinetics of Thermal Decomposition of Ammonium Perchlorate by TG/DSC-MS-FTIR. *J. Energ. Mater.* **2014**, *32*, 16–26.
- (22) Bhavanam, A.; Sastry, R. C. Kinetic study of solid waste pyrolysis using distributed activation energy model. *Bioresour. Technol.* **2015**, *178*, 126–131.
- (23) Wójtowicz, M. A.; Bassilakis, R.; Smith, W. W.; Chen, Y.; Carangelo, R. M. Modeling the evolution of volatile species during tobacco pyrolysis. *J. Anal. Appl. Pyrolysis* **2003**, *66*, 235–261.
- (24) Wu, W.; Mei, Y.; Zhang, L.; Liu, R.; Cai, J. Kinetics and reaction chemistry of pyrolysis and combustion of tobacco waste. *Fuel* **2015**, *156*, 71–80.
- (25) Zhao, D.; Dai, Y.; Chen, K.; Sun, Y.; Yang, F.; Chen, K. Effect of potassium inorganic and organic salts on the pyrolysis kinetics of cigarette paper. *J. Anal. Appl. Pyrolysis* **2013**, *102*, 114–123.
- (26) Barontini, F.; Tugnoli, A.; Cozzani, V.; Tetteh, J.; Jarriault, M.; Zinovik, I. Volatile products formed in the thermal decomposition of a tobacco substrate. *Ind. Eng. Chem. Res.* **2013**, *52*, 14984–14997.
- (27) Várhegyi, G.; Bobály, B.; Jakab, E.; Chen, H. Thermogravimetric study of biomass pyrolysis kinetics. A distributed activation energy model with prediction tests. *Energy Fuels* **2011**, *25*, 24–32.
- (28) Encinar, J. M.; Beltrán, F. J.; González, J. F.; Moreno, M. J. Pyrolysis of maize, sunflower, grape and tobacco residues. *J. Chem. Technol. Biotechnol.* **1997**, *70*, 400–410.
- (29) Chen, R.; Zhang, J.; Lun, L.; Li, Q.; Zhang, Y. Comparative study on synergistic effects in co-pyrolysis of tobacco stalk with polymer wastes: Thermal behavior, gas formation, and kinetics. *Bioresour. Technol.* **2019**, *292*, No. 121970.
- (30) Liao, J.; Lu, Z.; Hu, S.; Li, Q.; Che, L.; Chen, X. D. Effects of prewash on the pyrolysis kinetics of cut tobacco. *Drying Technol.* **2017**, *35*, 1368–1378.
- (31) Zhang, Y.; He, Q.; Cao, Y.; Bao, S.; Zhou, S.; Tian, Z.; Wang, X.; Peng, X.; Zhang, X.; Zhu, D.; She, S. Interactions of tobacco shred and other tobacco-based materials during co-pyrolysis and co-combustion. *J. Therm. Anal. Calorim.* **2019**, *136*, 1711–1721.
- (32) Luo, K.; Xing, J.; Bai, Y.; Fan, J. Universal Devolatilization Process Model for Numerical Simulations of Coal Combustion. *Energy Fuels* **2017**, *31*, 6525–6540.
- (33) Bridgwater, A. V.; Meier, D.; Radlein, D. An overview of fast pyrolysis of biomass. *Org. Geochem.* **1999**, *30*, 1479–1493.
- (34) Guo, J.; Shang, P.; Cai, J.; Zhao, L.; Liu, H.; Wang, H. Determination of hydrogen cyanide retention in cigarette filters with continuous flow analysis. *Zhongguo Yancao Xuebao* **2015**, *21*, 1–4.
- (35) Russow, R. W. B.; Intorp, M.; Mueller, C.; Stange, C. F. GC-RF-MS method to determine the <sup>13</sup>C abundance of gaseous combustion products in cigarette smoke. *Isot. Environ. Health Stud.* **2007**, *43*, 257–262.
- (36) Wang, H.; Guo, J.; Yin, Y.; Liu, S.; Zhao, X.; Xie, F.; Zhao, L. Determination of ammonia in sidestream cigarette smoke by continuous flow analysis method. *Yancao Keji* **2016**, *49*, 38–44.
- (37) Cardoso, C. R.; Miranda, M. R.; Santos, K. G.; Ataíde, C. H. Determination of kinetic parameters and analytical pyrolysis of tobacco waste and sorghum bagasse. *J. Anal. Appl. Pyrolysis* **2011**, *92*, 392–400.
- (38) Guo, G.; Liu, C.; Wang, Y.; Xie, S.; Zhang, K.; Chen, L.; Zhu, W.; Ding, M. Comparative investigation on thermal degradation of flue-cured tobacco with different particle sizes by a macro-thermogravimetric analyzer and their apparent kinetics based on distributed activation energy model. *J. Therm. Anal. Calorim.* **2019**, *138*, 3375–3388.
- (39) Valverde, J. L.; Curbelo, C.; Mayo, O.; Molina, C. B. Pyrolysis kinetics of tobacco dust. *Chem. Eng. Res. Des.* **2000**, *78*, 921–924.
- (40) Zhou, H.; Long, Y.; Meng, A.; Chen, S.; Li, Q.; Zhang, Y. A novel method for kinetics analysis of pyrolysis of hemicellulose, cellulose, and lignin in TGA and macro-TGA. *RSC Adv.* **2015**, *5*, 26509–26516.
- (41) Biagini, E.; Barontini, F.; Tognotti, L. Devolatilization of biomass fuels and biomass components studied by TG/FTIR technique. *Ind. Eng. Chem. Res.* **2006**, *45*, 4486–4493.

(42) Branca, C.; Albano, A.; Di Blasi, C. Critical evaluation of global mechanisms of wood devolatilization. *Thermochim. Acta* **2005**, *429*, 133–141.

(43) Mehrabian, R.; Scharler, R.; Obernberger, I. Effects of pyrolysis conditions on the heating rate in biomass particles and applicability of TGA kinetic parameters in particle thermal conversion modelling. *Fuel* **2012**, *93*, 567–575.